The Optimal FGM Design for Engine Manufacturing

Contents

Abstract

Due to the high requirements of engine materials design, a plate which obtains the capability to stand the high temperature difference between internal and external surface is expected. Considering the practical physical environment of ultra-highly condensed air inside the engine, people require certain level of ability to withstand the pressure. This could be satisfied by the thermal stress created with special design to defeat the great temperature difference.

Functionally Gradient Materials design can be applied to meet the need. FGM, abbreviated from Functionally Gradient Materials, is a category of new composition of two pure materials, with uniformly mixed components inside each layer. In our paper, the materials are designed to meet the above requirements. The internal side layer is made of pure metal of Aluminum, and the external side layer is made of pure Zirconia, which can defend the heat from getting inside. For the middle layers, a ratio of Aluminum is mixed into the materials, and the rest of the layer is Zirconia. Hence, a new material which obtains the strong elasticity and the high ability to withstand ultra-high temperature difference is created.

With the aid of simulation software the ANSYS, two models are established to test and identify the ability of the materials. The results are shown in the latter part of this paper. It is proved that this kind of design method is capable to satisfy the strict demands of both temperature and elasticity. At the same time, a new principle is found in our experiments on ANSYS modeling: the more layers the materials design contains, the better performance the plate will present. This principle is proved by our later comparison of four-layer plate and six-layer plate, with the same middle layer materials design schema.

Key words: FGM; Heat Conduction Equation; ANSYS

1 Introduction

Owing to the differences of thermal and mechanical properties in Zirconia and Aluminum, residual stresses develop in regions near the Zirconia/Aluminum interfaces during fabrication and under thermal and mechanical loading in service. These stresses affect performance and the lifetime of this kind of material and can cause cracking, which is unexpected in manufacturing industry. In order to solve this problem, a new category of mixed materials design schema is generated to satisfy the strict requirements. In this paper, two models are exhibited to demonstrate the capability of applying the new materials design schema.

The first model is established with 4 layers, the close-to-outer-edge layer is made of pure Zirconia to resist the high temperature and keep heat from conducting inside. The internal side layer is made of pure Aluminum (a category of Aluminum composition), which can present strong elasticity to offset the strength or pressure from physical force.

The second model is also created by the same principle, and with the same materials design schema. However, this one has 6 layers, and the middle 4 layers are using 4 different materials from the first one. The middle layers are made of materials of composition from the both involved.

The results from ANSYS 14.0 are shown below in the final part of analysis, which strictly demonstrate its features on satisfying the extreme condition of temperature difference. Besides, the exact indexes are the thermal stress and the temperature map of final state.

2 Problem Restatement

An engine company is developing a new kind of engine which has excellent working performance. And it can work at the condition with internal and external temperature of varying large difference.
Functional Gradient Materials (FGM) is a kind of composition within the structure of a continuous gradient variation of new heterogeneous composite materials. It can be widely used in many fields. So the engine will be made of FGM with different metal layers.
We need to give the reasonable analysis to the FGM with different metal layers and provide a model to the heat conduction. In addition, we are supposed to give a reasonable designing scheme of the FGM with different metal layers, which satisfying internal and external temperature of 550℃ and 80℃ respectively, referring to the common metal's heat

conducting relevant data.

3 Conventions

This section defines the basic terms used in this paper.

3.1 Terminology

・ Heat conductivity: It represents the coefficient of thermal conductivity, which means the quantity of heat conduct through cross sectional area in unit time when the temperature decrease for 1℃.

・ Young's modulus: It represents the physical quantity of the anti-pressure ability of the material within the elastic limit.

・ Coefficient of thermal expansion: It describes how the size of an object changes with a change in temperature. Specifically, it measures the fractional change in size per degree change in temperature at a constant pressure.

・ Poisson's ratio: It is the negative ratio of transverse to axial strain. When a material is compressed in one direction, it usually tends to expand in the other two directions perpendicular to the direction of compression.

・ ZL109: It is short for ZAlSi12Cu1Mg1Ni1, a category of Aluminum.

3.2 Variables

Symbols	definitions
$k(y)$	coefficient of thermal conductivity
$\rho(y)$	density of the material
$c(y)$	specific heat capacity
$T(y,t)$	function of temperature field

4 Assumptions

- The external side of the plate is touched by the air of room temperature of 20 Celsius.
- The internal and external temperatures are constant during the whole process of heat conducting and convection.
- In order to make better result, plates are formed with 4 round borders, which have a radius of 1mm to satisfy the width of 2 millimeter of the layer.
- The materials of each layer are uniformly mixed with both pure materials.

5 Model Ⅰ: The four-layer model

5.1 The foundation of Model Ⅰ

To simplify the problem, we begin our model with a four-layer composite material. And it's designed as follows:

- The first layer: metal--the pure ZL109 material made layer.
- The second layer: P_1% ZL109 + ($1-P_1$%) Zirconia.
- The third layer: P_2 % ZL109 + ($1-P_2$%) Zirconia ($1>P_1>P_2>0$).
- The fourth layer: anti-heat--the pure Zirconia.

For this four-layer composite material, the edge condition consists of the external surface and internal surface. We consider that the external surface can conduct heat and thermal convection, the internal surface is heat insulation. Hence, the heat conduction takes place inside the metal layers.

The transient heat conduction equation of this composite material:

$$\rho(y)c(y)\frac{\partial T(y,t)}{\partial t}=\frac{\partial}{\partial y}\left\{k(y)\frac{\partial T(y,t)}{\partial y}\right\} \qquad (1)$$

For the initial conditions and thermal convection conditions are:

$$t = 0, T = T_0$$
$$t > 0, \begin{Bmatrix} y = 0, k(y)\dfrac{\partial T(y,t)}{\partial y} - \xi_a T(y,t) = -\xi_a T_a \\ y = b, k(y)\dfrac{\partial T(y,t)}{\partial y} + \xi_b T(y,t) = \xi_b T_b \end{Bmatrix} \tag{2}$$

We solve the above equation by the finite element method. The corresponding functional can help to find the approximate solutions. The following functional is defined in $\Delta t_n (n = 1, 2, \cdots, \mathrm{N})$ [1]:

$$\pi = -\left\{ \int_{t_{n-1}}^{t_n} \left[\int_0^b \frac{1}{2} k(y) \left(\frac{\partial T(y,t)}{\partial y} \right)^2 + \rho(y) \frac{c(y)}{\Delta t_n} \left(\frac{T^2(y,t)}{2} - T_{n-1} T(y,t) \right) \right] dy + \int_{\Gamma}^{\xi} \left(\frac{T^2(y,t)}{2} - T_\Gamma T(y,t) \right) d\Gamma \right\} dt \tag{3}$$

where ξ is the convective heat transfer coefficient($y = 0, \xi = \xi_a; y = b, \xi = \xi_b$).

In the convective heat transfer boundary conditions, the finite element equation of transient heat conduction is [2]:

$$\left([\mathrm{H}] + [\mathrm{Q}] \right)(T) = \{P\} + [Q]\{T_{n-1}\} \tag{4}$$

where $[H]$ is the temperature stiffness matrix, $[\mathrm{Q}]$ is the temperature coefficient matrix, $\{T\}$ is the column vector of unknown temperature value. The elements of $[H], [\mathrm{Q}], \{P\}$ are as follows:

$$h_{rs}^e = \frac{k^e}{4\Delta^e}(b_r b_s + c_r c_s) + \frac{\xi^e}{3} s_{jk} \frac{1}{2}\left(1 + \delta_{rs}\right)\left(\delta_{rj} + \delta_{rk}\right)\left(\delta_{sj} + \delta_{sk}\right) \tag{5}$$

$$q_{rs}^e = \frac{\rho^e c^e \Delta^e}{6\Delta t_n} \frac{1}{2}\left(1 + \delta_{rs}\right) \tag{6}$$

$$p_s^e = \frac{\xi^e}{2} T_\Gamma s_{jk} (\delta_{sj} + \delta_{sk}) \tag{7}$$

Given the degree of accuracy and the stability, we choose the difference schemes of Galerkin, which can be described as follows:

$$\frac{2}{3}\left(\frac{\partial T}{\partial t}\right)_t + \frac{1}{3}\left(\frac{\partial T}{\partial t}\right)_{t-\Delta t} = \frac{1}{\Delta t}\left(T_t - T_{t-\Delta t}\right) + O\left(\Delta t^2\right) \tag{8}$$

5.2 Analysis and calculation

5.2.1 Property value of the material

The pure materials we take to form the Functional Gradient Materials are ZrO_2 and $\mathrm{Ti-Al-4V}$, their physical properties are in Table 1[3].

Table 1 Material properties of ZrO_2 and $\mathrm{Ti-Al-4V}$

Material	Thermal conductivity $/\mathrm{w.(m.K)^{-1}}$	Specific heat $/\mathrm{J.(kg.K)^{-1}}$	Density $/\mathrm{kg \cdot m^{-3}}$
ZrO_2	2.09	456.7	5331
$\mathrm{Ti-Al-4V}$	7.50	537.0	4420

The volume fraction and degree of porosity of the metal phase and ceramic phase in our paper are:

$$V_m(\bar{y}) = \begin{cases} 1-\bar{y}^M & M \geq 1 \\ (1-\bar{y})^{\frac{1}{M}} & M < 1 \end{cases} \qquad (9)$$

$$V_c(\bar{y}) = 1 - V_m(\bar{y})$$

$$P(\bar{y}) = A\bar{y}(1-\bar{y}) \quad 4 > A \geq 0 \qquad (10)$$

where $\bar{y} = y/b$, meaning we have eliminated the dimension .

And the property value of the FGM in our paper can be determined by the following formulas:

$$\begin{cases} \rho(\bar{y}) = \rho_0(1-P) + \rho_\alpha P \\ c(\bar{y}) = \{c_0\rho_0(1-P) + C_\alpha\rho_\alpha P\} / \{\rho_0(1-\rho) + \rho_\alpha P\} \\ k(\bar{y}) = \left[(1-P^{1/3})/k_0 + P^{1/3} / \{(1-P^{2/3})k_0 + P^{2/3}k_\alpha\}\right]^{-1} \end{cases} \qquad (11)$$

$$\begin{cases} k_0 = k_c + 3k_c(k_m - k_c)V_m / \{3k_c + (k_m - k_c)V_c\} \\ \rho_0 = \rho_m V_m + \rho_c V_c \\ c_0 = (c_m\rho_m V_m + c_c\rho_c V_c)/(\rho_m V_m + \rho_c V_c) \end{cases} \qquad (12)$$

5.2.2 Analysis of Temperature field

We divide the finite element grid into 5240 units and 24606 nodes.

In condition that $M = 1.0, T_b = 1300.0K$, the temperature inside the panel is

increasing along with the external temperature.(1300K equals to 550
We change the numerical value of M , and other parameters are invariant. The transient temperature distribution is changing along with the changing of M .

5.3 Solution to the model

In order to show the distribution of the heat across the outer edge of the four layers plates, we use ANSYS to do simulation.[4]
We use the following three figures to show the result of the first model. More details of this model are shown in the appendix attached at the last part of this paper.

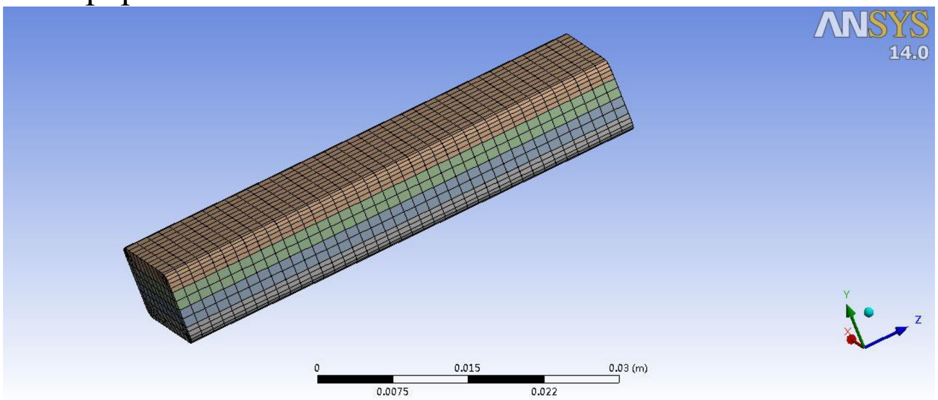

Figure 1 The grid chart of the four layers plates

The figure above clearly shows the first model, including its grid net and the 4 layers.

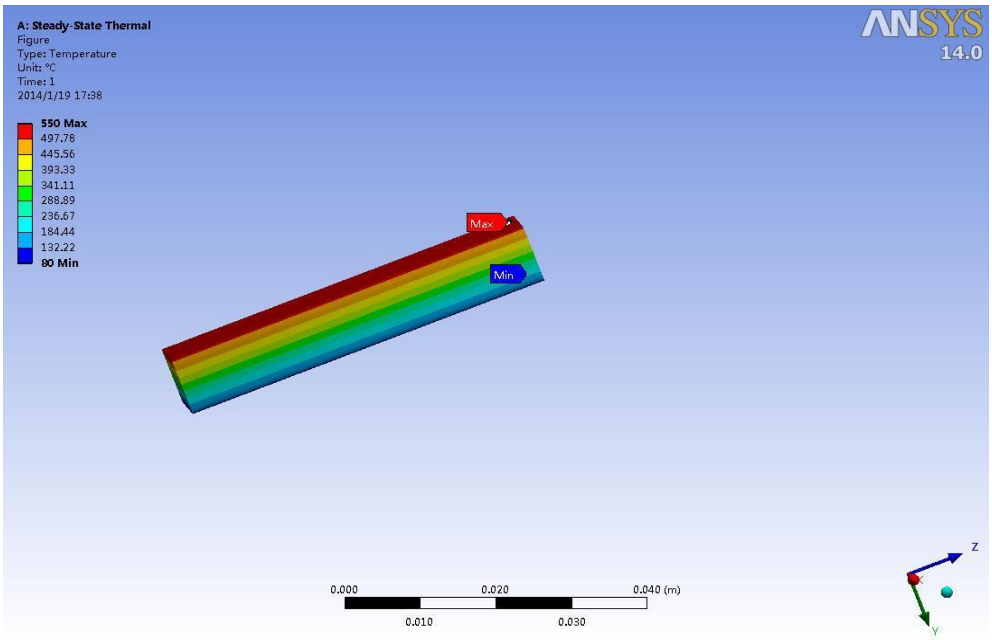

Figure 2 The temperature map of the four layer plates

The temperature map of this model after duration of heat conducting and surface convection is shown as in figure 2.

It is obviously that the external side is colder than the internal side, and the average temperature is estimated to be around 340 Celsius, which is an acceptable level. Due to the convection of the external surface contacting the air, the main part of the plate is keeping cool. This result seems fine and acceptable.

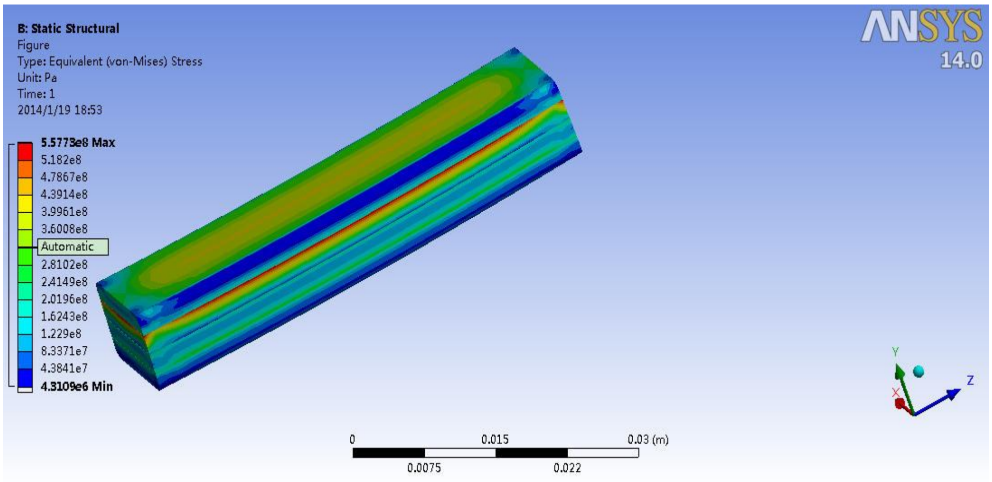

Figure 3 The thermal equivalent stress map

The maximum thermal stress is 5.5778e8, and the minimum is 4.3109e6. It can be checked that this stress is lower than the min allowable stress of this mixed material.

6 Model Ⅱ: The six-layer model

6.1 The foundation of Model Ⅱ

In this part, we use six-layer model to compare with the four-layer model. The six layers are composed with the following materials:

- The first layer: metal--the pure ZL109 material made layer.
- The second layer: P_1% ZL109 + ($1-P_1$%) Zirconia.
- The third layer: P_2 % ZL109 + ($1-P_2$%) Zirconia. (1>P_1>P_2>0).
- The fourth layer: P_3%ZL109 + ($1-P_3$%) Zirconia. (1>P_1>P_2>P_3>0)
- The fifth layer: P_4% ZL109 + (1-P_4%) Zirconia. (1>P_1>P_2>P_3>0).

- The sixth layer: anti-heat--the pure Zirconia.

All the parameters P_1, P_2, P_3 and P_4 can be determined by the following function[5][6]:

$$V_c = \left(\frac{2z+h}{2h}\right)^n \qquad -\frac{h}{2} \le z \le \frac{h}{2} \tag{13}$$

where h is the thickness of the structure, and n is a volume fraction exponent. Accordingly, the distribution of the modulus of elasticity an isotropic FGM and its Poison's ratio can be defined in terms of the material constants of the constituent phases based on a selected homogenization approach.
The parameters of the materials in the four-layer model can be determined by the above function as well.

The same as model Ⅰ, the transient heat conduction equation of this composite material:

$$\rho(y)c(y)\frac{\partial T(y,t)}{\partial t} = \frac{\partial}{\partial y}\left\{k(y)\frac{\partial T(y,t)}{\partial y}\right\} \tag{14}$$

For the initial conditions and thermal convection conditions are:

$$t = 0, T = T_0$$

$$t > 0, \left\{\begin{array}{l} y = 0, k(y)\dfrac{\partial T(y,t)}{\partial y} - \xi_a T(y,t) = -\xi_a T_a \\ y = b, k(y)\dfrac{\partial T(y,t)}{\partial y} + \xi_b T(y,t) = \xi_b T_b \end{array}\right\} \tag{15}$$

We solve the above equation by the finite element method which has explained in model Ⅰ.

6.2 Solution to the model

Using ANSYS 14.0, the model can be built by a few calculated or looked up arguments [7]:
The six-layer model with Fillet should meet the following to goals:

- Internal Temperature: Higher/ 550℃

- External Temperature: Lower/80℃

The table 2 shows the relative parameters of each layer about the six-layer model.

Table 2 The relative parameters

	Heat conductivity (kcal/m.h. ℃)	Young's Modulus(GPa)	Thermal Expansion Coefficient	Poisson's Ratio
The 1st layer	7.2	200	1.14e-5	0.310
The 2nd layer	62.640	112.9	1.92e-5	0.323
The 3rd layer	35.933	134.6	1.72e-5	0.320
The 4th layer	17.816	154.4	1.54e-5	0.317
The 5th layer	6.449	173.2	1.38e-5	0.314
The 6th layer	2.15	70	2.30e-5	0.330

And the following figures demonstrate that this design can reduce the maximum and the average temperature and thermal stress caused by temperature difference between internal side and external side.

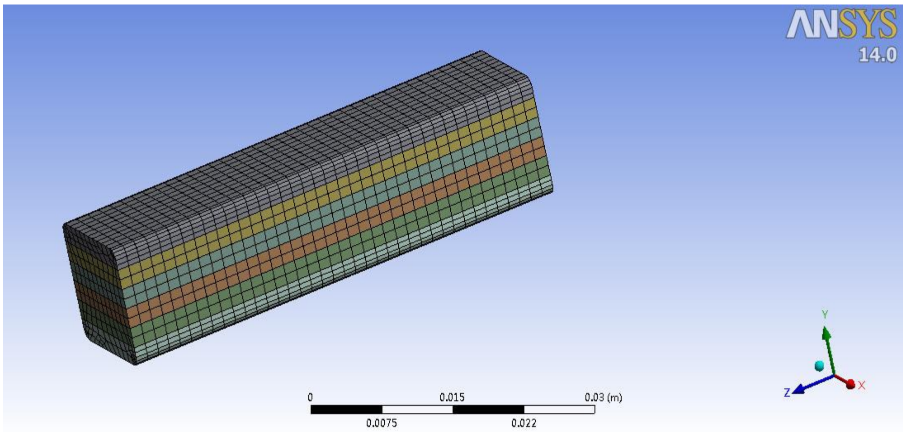

Figure 4 The grid chart of the six layers plates

Actually, the detail number of grid node is 31806, and there are 6954 elements inside the model.

It is built up by 6 clinging layers, they are all have the same width and height and length, but their materials are different from each other, which means they have rather differed specialties on thermal features directly determined by its physical properties.

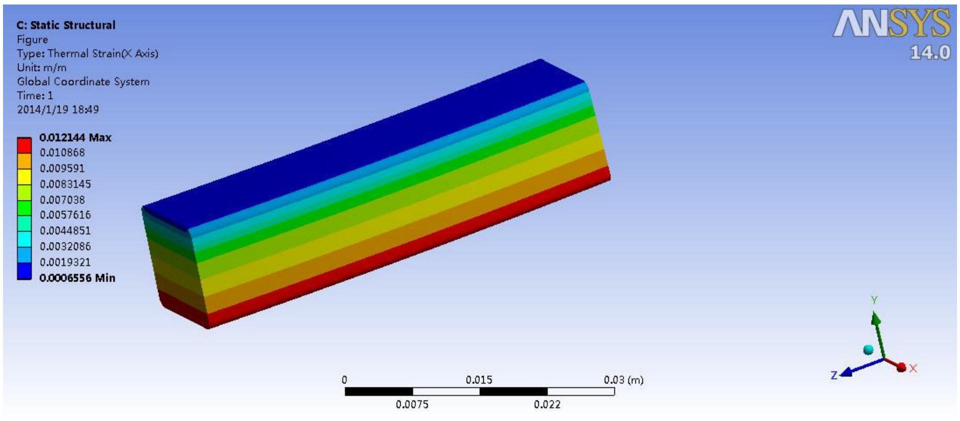

Figure 5 The thermal strain map of the six layers plates

The maximum thermal strain is 1.2144%. It is tiny, and absolutely won't effect the whole withstand ability.

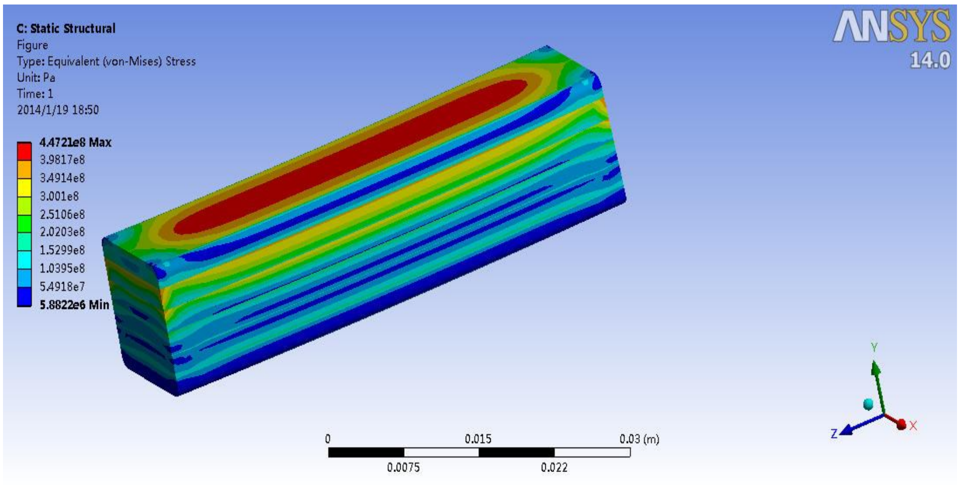

Figure 6 The thermal equivalent stress map of the six layers plates

It is obvious that the special corner suffering high stress disappeared from our result with fillet. Hence, it is strongly recommended to have fillet on shape design when applying this sort of materials design schema into the practical manufacturing process.

Seen from the figure above, the surface next the internal side is suffering biggest stress. The maximum value of Thermal Stress is 4.4721e8, which is much lower than the previous model of 4 layers.

According to the applying environment, the materials are required to withstand the higher temperature difference, which means they should have lower thermal stress, so this latter one of 6 layers, are proved to perform better.

7 Testing the results

When new schema of materials design is applied, better capability of withstanding temperature difference is demonstrated, and it can find the theoretical proof in the layer analysis.
For multi-layer plate, the materials are made of 2 completely different things; they own rather different physical properties, which can determine thermal behaviors under specialized condition of ultra-high temperature. On one hand, the Zirconia can prevent the heat from getting too fast into the metal, which means it can also keep heat inside the plate and won't let them out. This is a useful feature for engine design. One the other hand, the Aluminum is of great elastic ability, which will help to offset the stress created by the physical forces from touching objects.
Thus, the composite material has the two features that counts in engine manufacturing.

7.1 Sensitivity analysis

Experiments are conducted to demonstrate whether this optimization of the design schema can hold on with one side of the plate is of heat insulation; the result shows that the thermal stress increased a little less than 8 percent of original model, which means the original model, can be extended to the one-side-heat-insulation situation. When the corner of each plate is not filleted, the result still show clearly similar, only to find that the 4 corners are behaving badly on temperature and thermal stress, but not on thermal strain.

7.2 Specific results

We use the following table to show the specific results of the two models in our paper.

Table 3 Comparison of the two models

	The 4-layer model	The 6-layer model
Maximum value of the Thermal Stress	5.5773e+8 Pa	4.4721e+8 Pa
Minimum value of the Thermal Stress	4.3109e+6 Pa	5.8822e+6 Pa

According to our analysis, the six layers plates can withstand the higher temperature differences, and it is proved to be better.

8 Strengths and Weaknesses

The models in this paper can be applied in the engine manufacturing. They can help to promote the capability of withstanding temperature difference caused by thermal stress and improve the quality of heat keeping. These two are mostly treasured in engine materials design.

For the weaknesses, our models are restricted by two important factors: one is the method to calculating the physical properties of the uniformly mixed materials; the other is the ideal environment of convection.

As for the first restraint, physical properties can be testified by real experiment of actual materials.

On the second restraint, the real physical environment may have wind, fog or something else, which will strongly affect the convection of heat. Sometimes it will cool the plate down, or just keep the materials in high temperature. This is a complicated task to examine the real conditions for the materials.

9 conclusion

We present the material design schema in this part again:

- The next-to-high-temperature-side layer is metal.
- The opposite side is non-metal layer.
- The middle layers are designed with uniformly mixed metal and non-metal materials.

When we determine the material of each layer, the other thing to consider is the metal ratio. It is determined by the formula 13 in the paper. And the manufacturer can modify it accordingly to satisfy different situations of appliance.

This design schema works successfully on meeting the requirements of ultra-high temperature difference, and also has a good performance on heat keeping capability.

Reference

[1] Obata Y, Noda N. Unsteady thermal stresses in a functionally gradient material plate (Analysis of one-dimensional unsteady heat transfer problem. Trans.JSME, 1993, 59(590):1090-1096.

[2] Tanigawa Y, Akai T, Kawamura R. Transient heat conduction and thermal stress problems of a no homogeneous plate with temperature dependent material properties. Thermal stresses, 1996, 19:77-102.

[3] Victor Birman, Larry W. Byrd. Modeling and analysis of Functionally Graded Materials and structures. Applied Mechanics Reviews, 2007, 9(60):195-216.

[4] J. N .Reddy. Analysis of functionally graded plates. International Journal for Numerical Methods in Engineering, 2000, 47: 663-684.

[5] M. Grujicic, H. Zhao. Optimization of 316 stainless steel/alumina functionally graded material for reduction of damage induced by thermal residual stresses. Material Science and Engineering, 1998, 252:117-132.

[6] Mostapha Raki, Reza Alipour, Amirabbs Kamanbedast. Thermal Buckling of Thin Rectangular FGM Plate. World Applied Science Journal, 2012, 16(1):52-62.

[7] Touisif Ahmed, Muhammad Ziaur Qahman, Debasish Adhikary. Analysis of Al FGM as biomaterial of Artificial Human Femoral Bone and Compare with Ti-Al-V Alloy through Computational Study. Global Journal of Research in Engineering, 2013, 3(13): 332-341.

Appendix

1. The first 4-layer model, ANSYS report on layer materials:

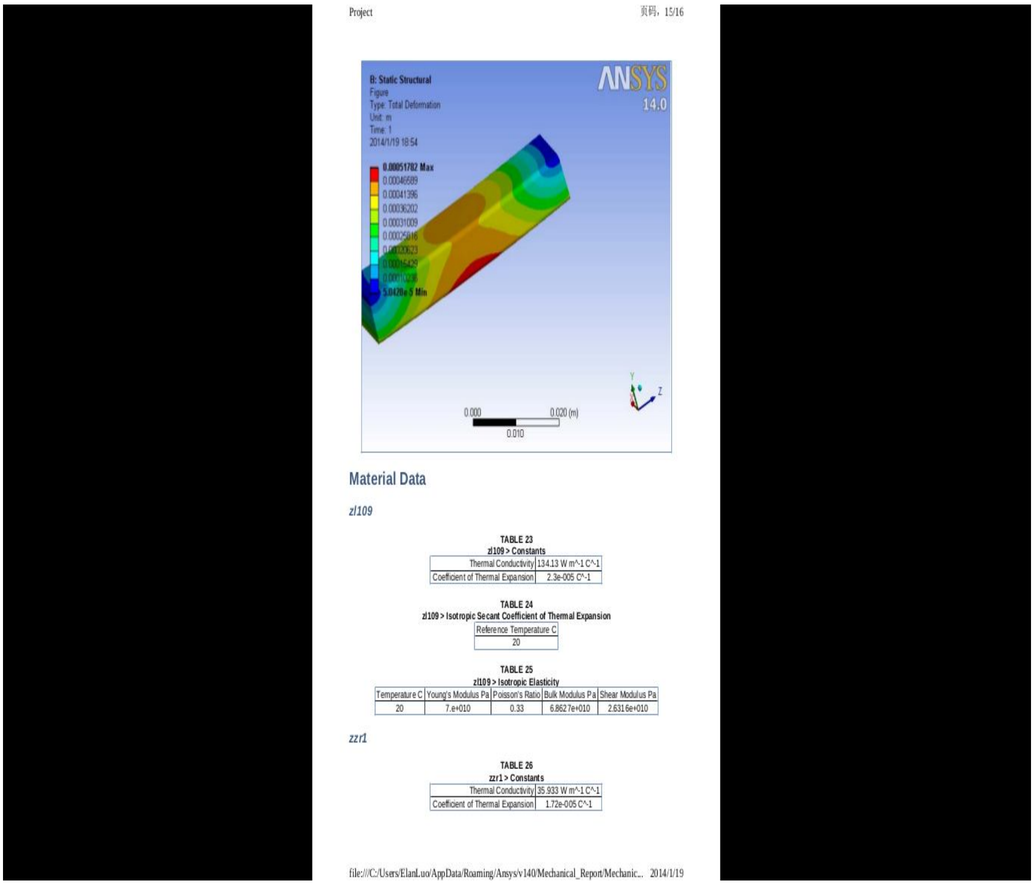

Project 页码，15/16

Material Data

zl109

TABLE 23
zl109 > Constants

Thermal Conductivity	134.13 W m^-1 C^-1
Coefficient of Thermal Expansion	2.3e-005 C^-1

TABLE 24
zl109 > Isotropic Secant Coefficient of Thermal Expansion

Reference Temperature C
20

TABLE 25
zl109 > Isotropic Elasticity

Temperature C	Young's Modulus Pa	Poisson's Ratio	Bulk Modulus Pa	Shear Modulus Pa
20	7.e+010	0.33	6.8627e+010	2.6316e+010

zzr1

TABLE 26
zzr1 > Constants

Thermal Conductivity	35.933 W m^-1 C^-1
Coefficient of Thermal Expansion	1.72e-005 C^-1

file:///C:/Users/ElanLuo/AppData/Roaming/Ansys/v140/Mechanical_Report/Mechanic... 2014/1/19

TABLE 27
zzr1 > Isotropic Secant Coefficient of Thermal Expansion

Reference Temperature C
20

TABLE 28
zzr1 > Isotropic Elasticity

Temperature C	Young's Modulus Pa	Poisson's Ratio	Bulk Modulus Pa	Shear Modulus Pa
20	1.346e+011	0.32	1.2463e+011	5.0985e+010

zzr2

TABLE 29
zzr2 > Constants

Thermal Conductivity	17.816 W m^-1 C^-1
Coefficient of Thermal Expansion	1.54e-005 C^-1

TABLE 30
zzr2 > Isotropic Secant Coefficient of Thermal Expansion

Reference Temperature C
20

TABLE 31
zzr2 > Isotropic Elasticity

Temperature C	Young's Modulus Pa	Poisson's Ratio	Bulk Modulus Pa	Shear Modulus Pa
20	1.544e+011	0.317	1.4062e+011	5.8618e+010

zro2

TABLE 32
zro2 > Constants

Thermal Conductivity	1.857 W m^-1 C^-1
Coefficient of Thermal Expansion	1.14e-005 C^-1

TABLE 33
zro2 > Isotropic Secant Coefficient of Thermal Expansion

Reference Temperature C
20

TABLE 34
zro2 > Isotropic Elasticity

Temperature C	Young's Modulus Pa	Poisson's Ratio	Bulk Modulus Pa	Shear Modulus Pa
20	2.e+011	0.31	1.7544e+011	7.6336e+010

2. The second 6-layer model, ANSYS report on layer materials:

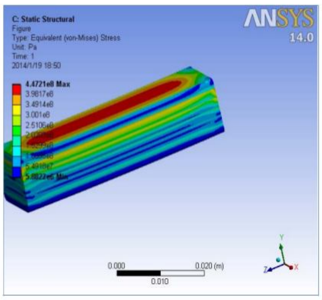

Material Data

zl109

TABLE 25
zl109 > Constants

Thermal Conductivity	134.13 W m^-1 C^-1
Coefficient of Thermal Expansion	2.3e-005 C^-1

TABLE 26
zl109 > Isotropic Secant Coefficient of Thermal Expansion

Reference Temperature C
20

TABLE 27
zl109 > Isotropic Elasticity

Temperature C	Young's Modulus Pa	Poisson's Ratio	Bulk Modulus Pa	Shear Modulus Pa
20	7.e+010	0.33	6.8627e+010	2.6316e+010

zzr3

TABLE 28
zzr3 > Constants

Coefficient of Thermal Expansion	1.92e-005 C^-1
Thermal Conductivity	62.64 W m^-1 C^-1

TABLE 29
zzr3 > Isotropic Secant Coefficient of Thermal Expansion

Reference Temperature C
20

TABLE 30
zzr3 > Isotropic Elasticity

Temperature C	Young's Modulus Pa	Poisson's Ratio	Bulk Modulus Pa	Shear Modulus Pa
20	1.129e+011	0.323	1.0631e+011	4.2668e+010

zzr1

TABLE 31
zzr1 > Constants

Thermal Conductivity	35.933 W m^-1 C^-1
Coefficient of Thermal Expansion	1.72e-005 C^-1

TABLE 32
zzr1 > Isotropic Secant Coefficient of Thermal Expansion

Reference Temperature C
20

TABLE 33
zzr1 > Isotropic Elasticity

Temperature C	Young's Modulus Pa	Poisson's Ratio	Bulk Modulus Pa	Shear Modulus Pa
20	1.346e+011	0.32	1.2463e+011	5.0985e+010

zzr2

TABLE 34
zzr2 > Constants

Thermal Conductivity	17.816 W m^-1 C^-1
Coefficient of Thermal Expansion	1.54e-005 C^-1

TABLE 35
zzr2 > Isotropic Secant Coefficient of Thermal Expansion

Reference Temperature C
20

TABLE 36
zzr2 > Isotropic Elasticity

Temperature C	Young's Modulus Pa	Poisson's Ratio	Bulk Modulus Pa	Shear Modulus Pa
20	1.544e+011	0.317	1.4062e+011	5.8618e+010

zzr4

TABLE 37
zzr4 > Constants

Coefficient of Thermal Expansion	1.38e-005 C^-1
Thermal Conductivity	6.449 W m^-1 C^-1

TABLE 38
zzr4 > Isotropic Secant Coefficient of Thermal Expansion

Reference Temperature C
20

TABLE 39

zzr4 > Isotropic Elasticity

Temperature C	Young's Modulus Pa	Poisson's Ratio	Bulk Modulus Pa	Shear Modulus Pa
20	1.732e+011	0.314	1.552e+011	6.5906e+010

zro2

TABLE 40
zro2 > Constants

Thermal Conductivity	1.857 W m^-1 C^-1
Coefficient of Thermal Expansion	1.14e-005 C^-1

TABLE 41
zro2 > Isotropic Secant Coefficient of Thermal Expansion

Reference Temperature C
20

TABLE 42
zro2 > Isotropic Elasticity

Temperature C	Young's Modulus Pa	Poisson's Ratio	Bulk Modulus Pa	Shear Modulus Pa
20	2.e+011	0.31	1.7544e+011	7.6336e+010